

Theoretical motivations and experimental signals for a second resonance of the Higgs field

Maurizio Consoli

INFN, Sezione di Catania, Italy

Seminarium Białasówka HEP/ HEP Seminar, Krakow 18 November 2022

References:

M.C., L. Cosmai, Int. J. Mod. Phys. **A35** (2020) 2050103; hep-ph/2006.15378

M.C., L. Cosmai, Symmetry **12** (2020) 2037; doi:103390/sym12122037

M.C. , in Veltman Memorial Volume, Acta Phys. Pol. **B52** (2021) 763; hep-ph/2106.06543

M.C., L. Cosmai, Int. J. Mod. Phys. **A37** (2022) 2250091; arXiv:2111.08962v2 [hep-ph]

M.C., L. Cosmai, F. Fabbri, arXiv:2208.00920 [hep-ph] (revised version November 2022)

Abstract

- 1) Theoretical arguments + lattice simulations give motivations for a relatively narrow, second resonance of the Higgs field with mass

$$(M_H)^{\text{THEOR}} = 690 \pm 10 \text{ (stat)} \pm 20 \text{ (sys) GeV}$$

produced at LHC mainly via gluon-gluon Fusion (ggF)

- 2) The ATLAS ggF 4-lepton events for invariant mass $m(4l)=530\div 830$ GeV, exhibit a (2.5- σ excess + 3.3- σ defect) suggesting the existence of a new resonance of mass $(M_H)^{\text{EXP}} \approx 700$ GeV

- 3) Other excesses suggesting a new resonance in the same mass region:

- i) ATLAS $\gamma\gamma$ events $\rightarrow 3.3 \sigma$ at 684(8) GeV

- ii) CMS (b-b + $\gamma\gamma$) channel $\rightarrow 1.6 \sigma$ at 675(25) GeV

- iii) CMS $\gamma\gamma$ produced in pp double-diffractive scattering $\rightarrow 3.3 \sigma$ at 650(40) GeV

- 4) Negligible correlation among these data
- 5) Having a definite prediction in some energy range, local significance should not be downgraded by the “look-elsewhere” effect
- 6) The present situation is unstable because the cumulated statistical evidence has reached the traditional 5-sigma discovery level

Presently accepted view: the mass spectrum of the Higgs field consists of a single narrow resonance of mass $\mathbf{m}_h = 125 \text{ GeV}$

At present, the excitation spectrum of the Higgs field is described in terms of a single narrow resonance of mass $m_h = 125 \text{ GeV}$ associated with the quadratic shape of the effective potential at its minimum. In a description of Spontaneous Symmetry Breaking (SSB) as a second-order phase transition, this point of view is well summarized in the review of the Particle Data Group [1] where the scalar potential is expressed as

$$V_{\text{PDG}}(\varphi) = -\frac{1}{2}m_{\text{PDG}}^2\varphi^2 + \frac{1}{4}\lambda_{\text{PDG}}\varphi^4 \quad (1)$$

By fixing $m_{\text{PDG}} \sim 88.8 \text{ GeV}$ and $\lambda_{\text{PDG}} \sim 0.13$, this has a minimum at $|\varphi| = \langle\Phi\rangle \sim 246 \text{ GeV}$ and a second derivative $V''_{\text{PDG}}(\langle\Phi\rangle) \equiv m_h^2 = (125 \text{ GeV})^2$.

- $\lambda_{\text{PDG}} \approx L^{-1}$ with $L \approx \ln(\Lambda_S)$
- $m_h^2 \approx \lambda_{\text{PDG}} \langle\Phi\rangle^2 \approx L^{-1} \langle\Phi\rangle^2$
- Infinitesimal quadratic shape $(V''_{\text{PDG}}(\langle\Phi\rangle) / \langle\Phi\rangle^2) \approx L^{-1} \rightarrow 0$ if $\Lambda_S \rightarrow \infty$
- Infinitesimal depth $(V_{\text{PDG}}(\langle\Phi\rangle) / \langle\Phi\rangle^4) \approx L^{-1} \rightarrow 0$ if $\Lambda_S \rightarrow \infty$

Some basic inconsistency?

- Now, vanishing quadratic shape \rightarrow free-field fluctuations = " Triviality "
- But RG-invariance of $V_{\text{eff}}(\varphi)$

$$\left(\Lambda_s \frac{\partial}{\partial \Lambda_s} + \Lambda_s \frac{\partial \lambda}{\partial \Lambda_s} \frac{\partial}{\partial \lambda} + \Lambda_s \frac{\partial \varphi}{\partial \Lambda_s} \frac{\partial}{\partial \varphi} \right) V_{\text{eff}}(\varphi, \lambda, \Lambda_s) = 0 \quad (17)$$

$$\Lambda_s \frac{\partial \varphi}{\partial \Lambda_s} \equiv \gamma(\lambda) \varphi$$

- No anomalous dimension at the minimum for $V_{\text{eff}}(\langle \Phi \rangle)$
- Vacuum energy density $V_{\text{eff}}(\langle \Phi \rangle)$ should be RG-invariant
- Otherwise, why should $\langle \Phi \rangle$ be Λ_s - independent ?
- Different scheme for the effective potential?

- Standard picture

$$V_{\text{PDG}}(\varphi) = -\frac{1}{2}m_{\text{PDG}}^2\varphi^2 + \frac{1}{4}\lambda_{\text{PDG}}\varphi^4$$

a classical, double-well potential with perturbative quantum corrections.

Traditional 2nd-order phase transition. Is this so obvious?

- For instance, in the presence of gauge bosons, SSB is a (weak) first-order phase transition (the Coleman-Weinberg massless limit corresponds to the broken phase). What about the **cutoff version** of pure Φ^4 (in 4D)?

This is better explained by the toy model

$$V_{\text{toy}}(\varphi) = \frac{1}{2}m^2\varphi^2 + \frac{1}{4!}\lambda\varphi^4 (1 + \epsilon \ln \varphi^2/\mu^2) \quad (4)$$

where μ is some mass scale and ϵ is a small parameter. (The real case is like $\epsilon \sim \lambda$ but here we treat ϵ as a separate parameter.) For $\epsilon = 0$, as one varies the m^2 parameter, one has a second-order phase transition, occurring at $m^2 = 0$. However, for any positive ϵ no matter how small, one has a first-order transition, occurring at a positive $m^2 = m_c^2$. Both the critical m_c^2 and the minimum are exponentially small $\mu^2 \exp(-1/\epsilon)$. This toy model illustrates that an infinitesimally weak first-order phase transition becomes indistinguishable from a second-order transition if one does not look on a fine enough scale.

- Lattice simulations \rightarrow (weak) 1st order phase transition

Ising limit of Φ^4 in 4D, traditionally adopted for lattice simulations, (e.g. Lüscher&Weisz) \rightarrow Landau pole at the lattice size

A non-trivial spectrum for the trivial $\lambda\phi^4$ theory

F. Gliozzi^a

^aDipartimento di Fisica Teorica, Università di Torino,
via P. Giuria 1, 10125 Torino, Italy

$$\log(\Lambda/m_r) \leq A/g_r + B \log(g_r) + C + \dots \quad (1)$$

$$S_\phi = \beta S_{links} + \sum_{x \in \mathcal{L}} (\phi_x^2 + \lambda(\phi_x^2 - 1)^2)$$

$$S_{links} = - \sum_{x \in \mathcal{L}} \sum_{\mu=1}^4 \phi_x \phi_{x+\hat{\mu}}$$

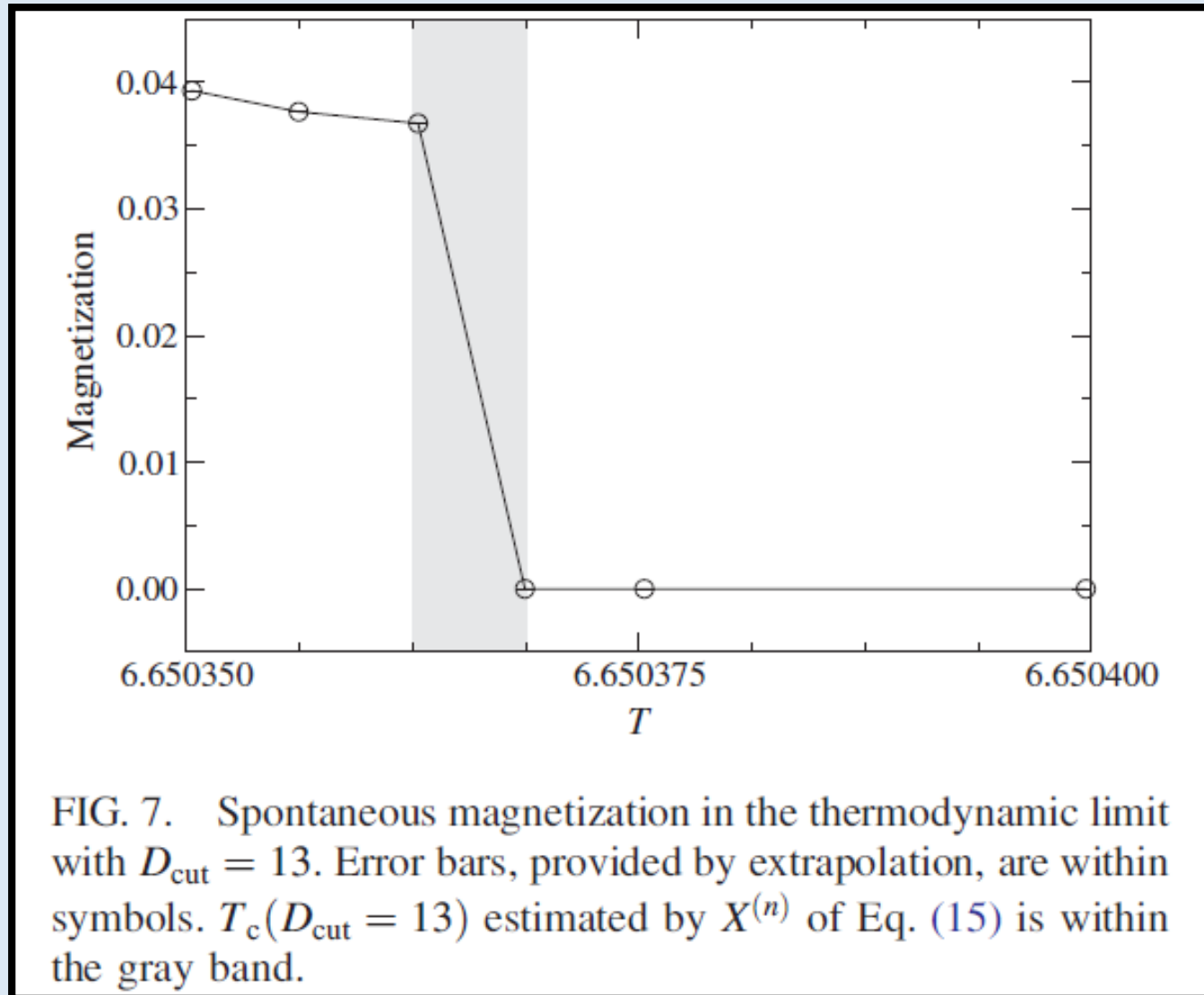
Where ϕ is a real field associated to the nodes x of the lattice and $\hat{\mu}$ denotes the unit vector in the μ -direction. Once m_r and g_r have been fixed, the renormalization group trajectories (the “lines of constant physics”) in the plane of the bare parameters flow toward higher values of the bare quartic coupling λ and terminate at the $\lambda \rightarrow \infty$ limit [5], where the action (2) reduces to that of the Ising model (3) with $\phi_x \in \pm 1$. In other terms, the 4D Ising model is the limit theory which saturates the the triviality bound (1): at fixed g_r is the best approximation to the continuum limit .



SSB in **cutoff Φ^4** \rightarrow weak first-order phase transition (see

P.H. Lundow and K. Markström, PRE 80(2009)031104; NPB 845(2011)120)

Picture below from S. Akiyama et al. PRD 100(2019)054510)



SSB in pure Φ^4 as a weak 1st-order transition means that the massless theory is in the broken phase as in the 1-loop and Gaussian potential. These have **2** mass scales: **m_h from quadratic shape of $V_{\text{eff}}(\varphi = \pm v)$ and M_H from zero-point energy**

By introducing the mass-squared parameter $M^2(\varphi) \equiv \frac{1}{2}\lambda\varphi^2$, the 1-loop potential can be expressed as a classical background + zero-point energy of a particle with mass $M(\varphi)$, i.e.

$$V_{1\text{-loop}}(\varphi) = \frac{\lambda\varphi^4}{4!} - \frac{M^4(\varphi)}{64\pi^2} \ln \frac{\Lambda_s^2 \sqrt{e}}{M^2(\varphi)} \quad (9)$$

Thus, non-trivial minima of $V_{\text{eff}}(\varphi)$ occur at those points $\varphi = \pm v$ where

$$M_H^2 = \frac{\lambda v^2}{2} = \Lambda_s^2 \exp\left(-\frac{32\pi^2}{3\lambda}\right) \quad (10)$$

with a quadratic shape

$$m_h^2 \equiv V''_{1\text{-loop}}(\pm v) = \frac{\lambda^2 v^2}{32\pi^2} = \frac{\lambda}{16\pi^2} M_H^2 \sim \frac{M_H^2}{L} \ll M_H^2 \quad (11)$$

where $L \equiv \ln \frac{\Lambda_s}{M_h}$. Notice that the energy density depends on M_h and *not* on m_h , because

$$\mathcal{E}_{1\text{-loop}} = V_{1\text{-loop}}(\pm v) = -\frac{M_H^4}{128\pi^2} \quad (12)$$

therefore the critical temperature at which symmetry is restored, $k_B T_c \sim M_H$, and the stability of the broken phase depends on the larger M_H and not on the smaller m_h .

$$V_G(\varphi) = \frac{\hat{\lambda}\varphi^4}{4!} - \frac{\Omega^4(\varphi)}{64\pi^2} \ln \frac{\Lambda_s^2 \sqrt{e}}{\Omega^2(\varphi)}$$

$$\hat{\lambda} = \frac{\lambda}{1 + \frac{\lambda}{16\pi^2} \ln \frac{\Lambda_s}{\Omega(\varphi)}}$$

$$\Omega^2(\varphi) = \frac{\hat{\lambda}\varphi^2}{2}$$

$$M_H^2 = \Omega^2(v)$$

$$\mathcal{E}_G = V_G(\pm v) = -\frac{M_H^4}{128\pi^2}$$

In both approximations

$$m_h^2 \equiv V''_{\text{eff}}(\pm v) \sim \frac{M_H^2}{L} \ll M_H^2$$

$m_h \neq M_H \rightarrow$ propagator $G(p)$ has not a single-pole structure

m_h^2 , being $V''_{\text{eff}}(\varphi)$ at the minimum, is directly the 2-point, self-energy function $|\Pi(p=0)|$.

On the other hand, the Zero-Point Energy (ZPE) is (one-half of) the trace of the logarithm of the inverse propagator $G^{-1}(p) = (p^2 - \Pi(p))$. After subtracting constant terms and quadratic divergences, matching the 1-loop zero-point energy at the minimum gives the relation

$$ZPE \sim -\frac{1}{4} \int_{p_{\min}}^{p_{\max}} \frac{d^4p}{(2\pi)^4} \frac{\Pi^2(p)}{p^4} \sim -\frac{\langle \Pi^2(p) \rangle}{64\pi^2} \ln \frac{p_{\max}^2}{p_{\min}^2} \sim -\frac{M_H^4}{64\pi^2} \ln \frac{\Lambda_s^2}{M_H^2} \quad (3)$$

This shows that M_H^2 effectively refers to some average value $|\langle \Pi(p) \rangle|$ at larger p^2 .

\rightarrow Therefore, if $m_h \neq M_H$, there must be a non-trivial momentum dependence of $\Pi(p)$ \leftarrow

Check with lattice simulations of the scalar propagator.

Lattice simulations of the scalar propagator



ELSEVIER

Available online at www.sciencedirect.com

SCIENCE @ DIRECT®

Nuclear Physics B 729 [FS] (2005) 542–557

NUCLEAR
PHYSICS B

Comparison of perturbative RG theory with lattice data for the 4d Ising model

P.M. Stevenson

$$S = \sum_x \left[-2\kappa \sum_{\mu=1}^4 \phi(x)\phi(x + \hat{\mu}) + \phi(x)^2 + \lambda(\phi(x)^2 - 1)^2 \right], \quad (1)$$

which is equivalent to the more traditional expression

$$S = \sum_x \left[\frac{1}{2} \sum_{\mu=1}^4 (\partial_{\mu}\phi_0(x))^2 + \frac{1}{2}m_0^2\phi_0(x)^2 + \frac{g_0}{4!}\phi_0^4 \right], \quad (2)$$

where $\partial_{\mu}\phi_0(x) = \phi_0(x + \hat{\mu}) - \phi_0(x)$. The translation between the two formulations is given by

$$\phi_0 = \sqrt{2\kappa}\phi, \quad m_0^2 = \frac{(1 - 2\lambda)}{\kappa} - 8, \quad g_0 = \frac{6\lambda}{\kappa^2}. \quad (3)$$

Stevenson's analysis of the lattice propagator

(data from Balog, Duncan, Willey, Niedermeyer, Weisz NPB714(2005)256)

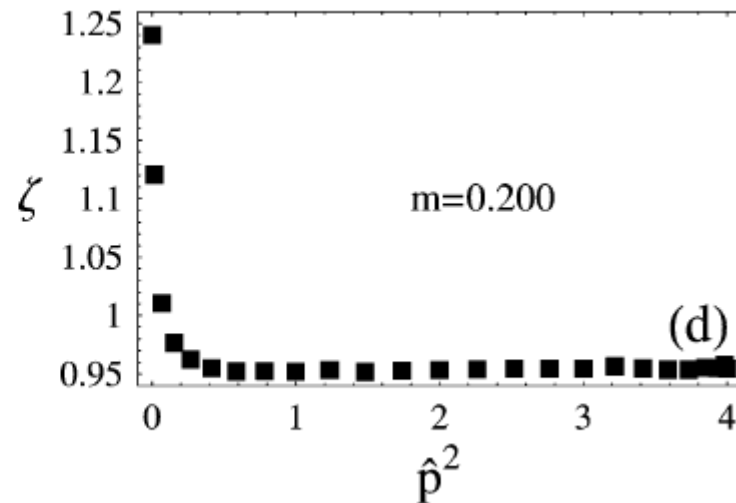
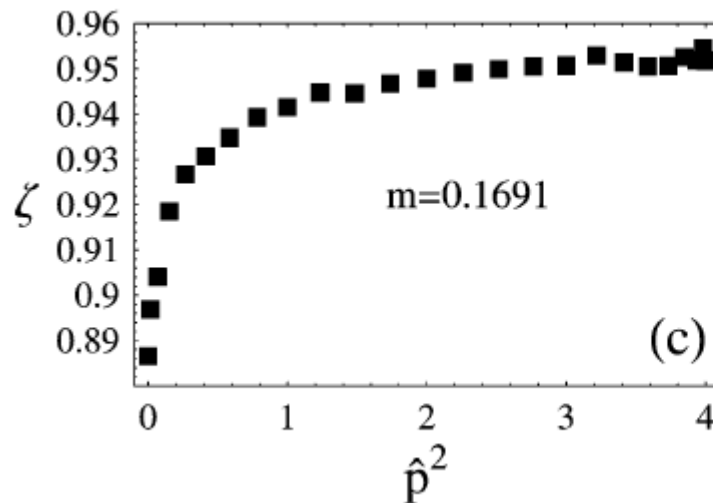
For $\kappa=0.0751$ in the broken phase, he reports the rescaled propagator data.

$$\zeta \equiv (\hat{p}^2 + m^2)G(p)$$

Standard one-pole propagator $\rightarrow \zeta$ has a flat profile

Left: re-scaling with the mass 0.1691 from the $p=0$ limit

Right: re-scaling with the mass giving a flat profile at larger p^2



Lattice Checks

(M.C. and Leonardo Cosmai, Int. J. Mod. Phys. A35 (2020) 2050103; hep-ph/2006.15378)

- A consistency check: no two-mass structure in the symmetric phase

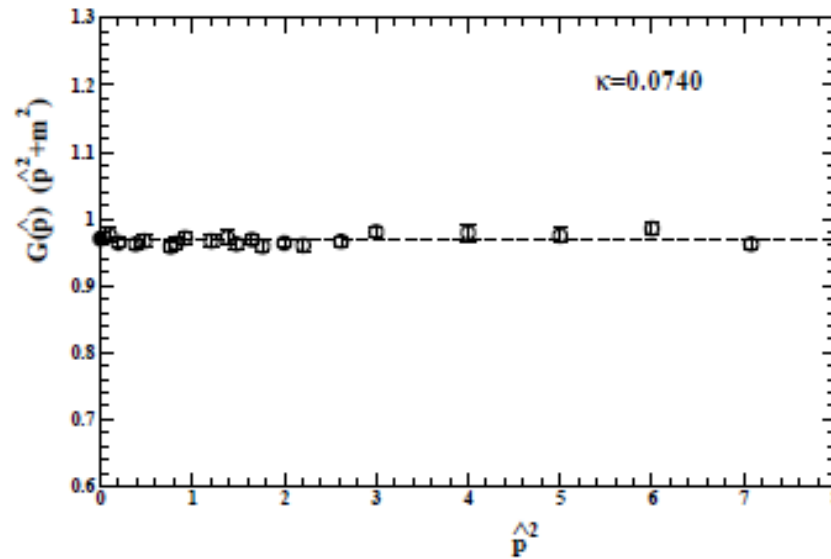
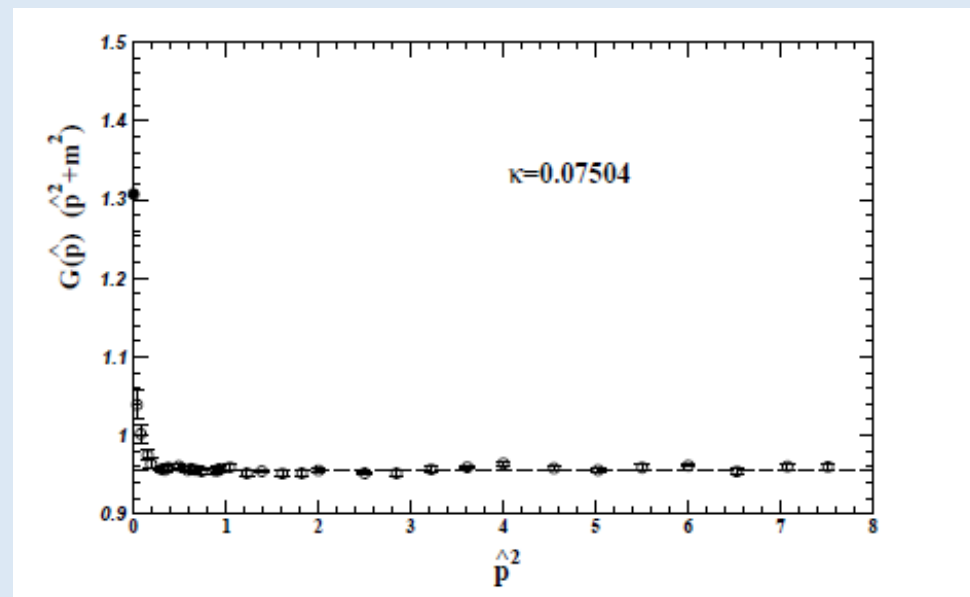
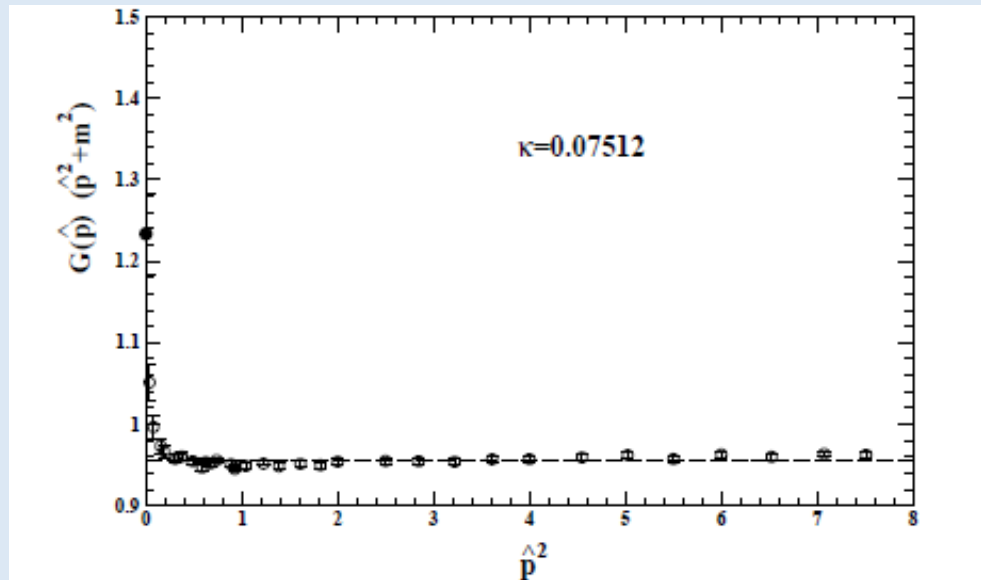


Figure 1: *The lattice data of ref.[8] for the re-scaled propagator in the symmetric phase at $\kappa = 0.074$ as a function of the square lattice momentum \hat{p}^2 . The fitted mass from high \hat{p}^2 , $m_{\text{latt}} = 0.2141(28)$, describes well the data down to $\hat{p} = 0$. The dashed line indicates the value of $Z_{\text{prop}} = 0.9682(23)$ and the $\hat{p} = 0$ point is $2\kappa\chi m_{\text{latt}}^2 = 0.9702(91)$.*

Lattice propagator in the broken phase

(P.Cea., M.C, L.Cosmai, P.M.Stevenson, MPLA14(1999)1673)



Propagator on a 76^4 lattice: 2 flat ranges \rightarrow 2 mass-shell regions

(M.C. and L.Cosmai, IJMP A35 (2020) 2050103; hep-ph/2006.15378)

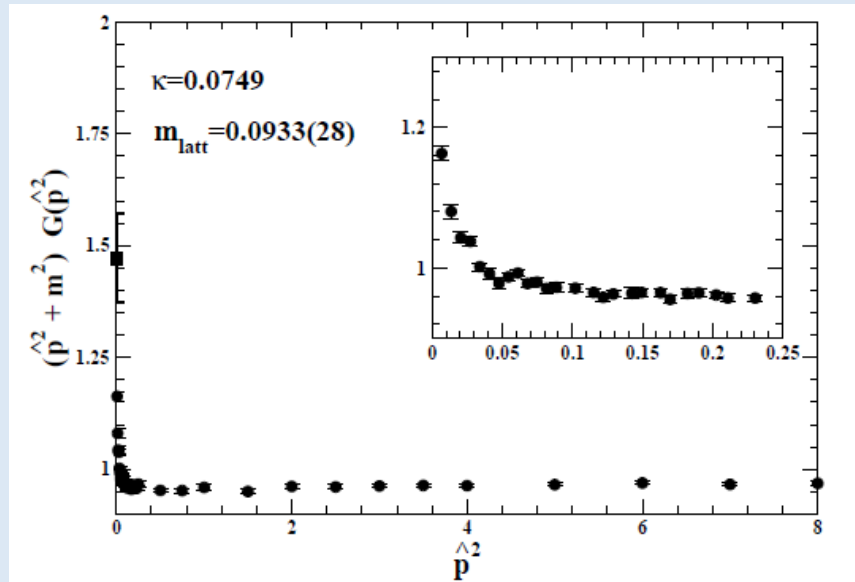


Figure 2: The propagator data of ref.[8], for $\kappa = 0.0749$, rescaled with the lattice mass $M_H \equiv m_{\text{latt}} = 0.0933(28)$ obtained from the fit to all data with $\hat{p}^2 > 0.1$. The peak at $p = 0$ is $M_H^2/m_h^2 = 1.47(9)$ as computed from the fitted M_H and $m_h = (2\kappa\chi)^{-1/2} = 0.0769(8)$.

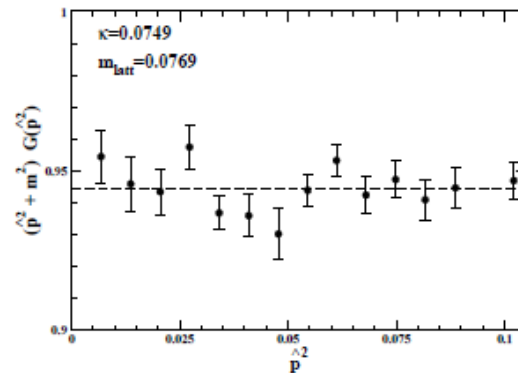


Figure 3: The propagator data of ref.[8] at $\kappa = 0.0749$ for $\hat{p}^2 < 0.1$. The lattice mass used here for the rescaling was fixed at the value $m_h = (2\kappa\chi)^{-1/2} = 0.0769(8)$.

Two-mass structure of the lattice propagator

By computing m_h^2 from the $p \rightarrow 0$ limit of $G(p)$ and M_H^2 from its behaviour at higher p^2 , the lattice data are consistent with a transition between two different regimes. By analogy with superfluid He-4, where the observed energy spectrum arises by combining the two quasi-particle spectra of phonons and rotons, the lattice data were well described in the full momentum region by the model form [7]

$$G(p) \sim \frac{1 - I(p)}{2} \frac{1}{p^2 + m_h^2} + \frac{1 + I(p)}{2} \frac{1}{p^2 + M_h^2} \quad (4)$$

with an interpolating function $I(p)$ which depends on an intermediate momentum scale p_0 and tends to $+1$ for large $p^2 \gg p_0^2$ and to -1 when $p^2 \rightarrow 0$. Most notably, the lattice data were also consistent with the expected increasing logarithmic trend $M_H^2 \sim Lm_h^2$ when approaching the continuum limit ³.

**The proportionality relation between M_H and $\langle\Phi\rangle \approx 246 \text{ GeV} \rightarrow$
The large M_H (and not the small m_h) determines vacuum stability. Thus, SSB could originate in the pure scalar sector, regardless of the other parameters of the theory**

Since, differently from m_h , the larger M_H would remain finite in units of the weak scale $\langle\Phi\rangle \sim 246.2 \text{ GeV}$ for an infinite ultraviolet cutoff, one can derive their proportionality relation. To this end, let us express M_H^2 in terms of $m_h^2 L$ through some constant c_2 , say

$$M_H^2 = m_h^2 L \cdot (c_2)^{-1} \quad (5)$$

and replace the leading-order estimate $\lambda \sim 16\pi^2/(3L)$ in the relation $\lambda = 3m_h^2/\langle\Phi\rangle^2$. Then M_H and $\langle\Phi\rangle$ are related through a cutoff-independent constant K

$$M_H = K \langle\Phi\rangle \quad (6)$$

with $K \sim (4\pi/3) \cdot (c_2)^{-1/2}$.

Estimating M_H from lattice simulations

Table 5: The values of M_H , as obtained from a direct fit to the higher-momentum propagator data. The two entries at $\kappa = 0.0749$, from our new simulations on a 76^4 lattice, refer to higher-momentum fits for $\hat{p}^2 > 0.1$ and $\hat{p}^2 > 0.2$ respectively. In the last column we report the combination $(c_2)^{-1/2} \equiv M_H \cdot (m_h)^{-1} \cdot [\ln(\Lambda_s/m_{M_H})]^{-1/2}$.

κ	M_H	$(m_h)^{-1}$	$[\ln(\Lambda_s/M_H)]^{-1/2}$	$(c_2)^{-1/2}$
0.07512	0.2062(41)	5.386(23)	0.606(2)	0.673(14)
0.0751	~ 0.200	5.568(16)	~ 0.603	~ 0.671
0.07504	0.1723(34)	6.636(32)	0.587(2)	0.671(14)
0.0749	0.0933(28)	13.00(14)	0.533(2)	0.647(20)
0.0749	0.100(6)	13.00(14)	0.538(4)	0.699(42)

- $(c_2)^{-1/2} = 0.67 \pm 0.01$ (stat) ± 0.02 (sys)
- $\mathbf{K} \equiv (4/3)\pi(c_2)^{-1/2} = 2.81 \pm 0.04$ (stat) ± 0.08 (sys)
- $\mathbf{M}_H = \mathbf{K} \langle \Phi \rangle = 690 \pm 10$ (stat) ± 20 (sys) GeV

Comparison with the traditional upper bounds on the mass of the first resonance

- The basic relations of our picture are $(L = \ln(\Lambda_s/M_H))$

$$\lambda \sim L^{-1} \quad m_h^2 \sim \langle \Phi \rangle^2 \cdot L^{-1} \quad M_H^2 \sim L \cdot m_h^2 = K^2 \langle \Phi \rangle^2 \quad (2)$$

- Thus from the third relation in (2) we deduce $m_h \ll M_H$ for a very large L . But M_H is cutoff independent. Therefore, by decreasing L , M_H remains fixed but m_h increases and approaches its maximum value $(m_h)^{\max} \approx M_H$ for $L \sim 1$, i.e. for a cutoff Λ_s which is a few times M_H
- Therefore this maximum value of m_h corresponds to

$$(m_h)^{\max} \sim (M_H)^{\text{Theor}} = 690 \pm 10 \text{ (stat)} \pm 20 \text{ (sys) GeV}$$

in good agreement with the upper bound obtained from the more conventional first two relations in Eq.(2)

$$(m_h)^{\max} = 670 \text{ (80) GeV,}$$

See Lang's complete review arXiv:hep-lat/9312004

- Viceversa, without performing our lattice simulations, we could have predicted $(M_H)^{\text{Theor}} = 670 \text{ (80) GeV}$ by combining the cutoff independence of M_H , the third relation in Eq.(2) and Lang's estimate of $(m_h)^{\max}$

Basic phenomenology of the heavy resonance. I

A heavy Higgs resonance H , with mass $M_H = K\langle\Phi\rangle \sim 700$ GeV, is usually believed to be a broad resonance due to the strong interactions in the scalar sector. This view derives from the original Lee-Quigg-Tacker calculation in the unitary gauge showing that, with a mass M_H in the scalar propagator, high-energy $W_L W_L$ scattering is indeed similar to $\chi\chi$ Goldstone boson scattering with a large contact coupling $\lambda_0 = 3K^2$. The same coupling would also enter the $H \rightarrow W_L W_L$ decay width.

However, by accepting the “triviality” of Φ^4 theories in 4D, the Λ –independent combination $3M_H^2/\langle\Phi\rangle^2 = 3K^2$ *cannot* represent a coupling entering observable processes. Indeed, the constant $3K^2$ is basically different from the coupling λ governed by the β –function

$$\ln \frac{\mu}{\Lambda} = \int_{\lambda_0}^{\lambda} \frac{dx}{\beta(x)} \quad (8)$$

For $\beta(x) = 3x^2/(16\pi^2) + O(x^3)$, whatever the contact coupling λ_0 at the asymptotically large Λ , at finite scales $\mu \sim M_H$ this gives $\lambda \sim 16\pi^2/(3L)$ with $L = \ln(\Lambda/M_H)$.

Basic phenomenology of the heavy resonance. II

Therefore, to find the $W_L W_L$ scattering amplitude at some scale μ , one should improve on the Lee-Quigg-Tacker calculation and first use the β -function to re-sum the higher-order effects in $\chi\chi$ scattering

$$A(\chi\chi \rightarrow \chi\chi) \Big|_{g_{\text{gauge}}=0} \sim \lambda \sim \frac{1}{\ln(\Lambda_s/\mu)} \quad (9)$$

and then use the Equivalence Theorem [18, 19, 20] which gives

$$A(W_L W_L \rightarrow W_L W_L) = [1 + O(g_{\text{gauge}}^2)] A(\chi\chi \rightarrow \chi\chi) \Big|_{g_{\text{gauge}}=0} = O(\lambda) \quad (10)$$

Thus the large coupling $\lambda_0 = 3K^2$ is actually replaced by the much smaller coupling

$$\lambda = \frac{3m_h^2}{\langle\Phi\rangle^2} = 3K^2 \frac{m_h^2}{M_H^2} \sim 1/L \quad (11)$$

M_H : heavy but relatively narrow resonance (produced mainly by the gluon-gluon Fusion mechanism)

For the same reason, the conventional large width into longitudinal vector bosons computed with $\lambda_0 = 3K^2$, say $\Gamma^{\text{conv}}(H \rightarrow W_L W_L) \sim M_H^3 / \langle \Phi \rangle^2$, should instead be rescaled by $(\lambda/3K^2) = m_h^2/M_H^2$. This gives

$$\Gamma(H \rightarrow W_L W_L) \sim \frac{m_h^2}{M_H^2} \Gamma^{\text{conv}}(M_H \rightarrow W_L W_L) \sim M_H \frac{m_h^2}{\langle \Phi \rangle^2} \quad (12)$$

where M_H indicates the available phase space in the decay and $m_h^2/\langle \Phi \rangle^2$ the interaction strength. If the heavier state couples to longitudinal W's with the same typical strength of the low-mass state it would represent a relatively narrow resonance.

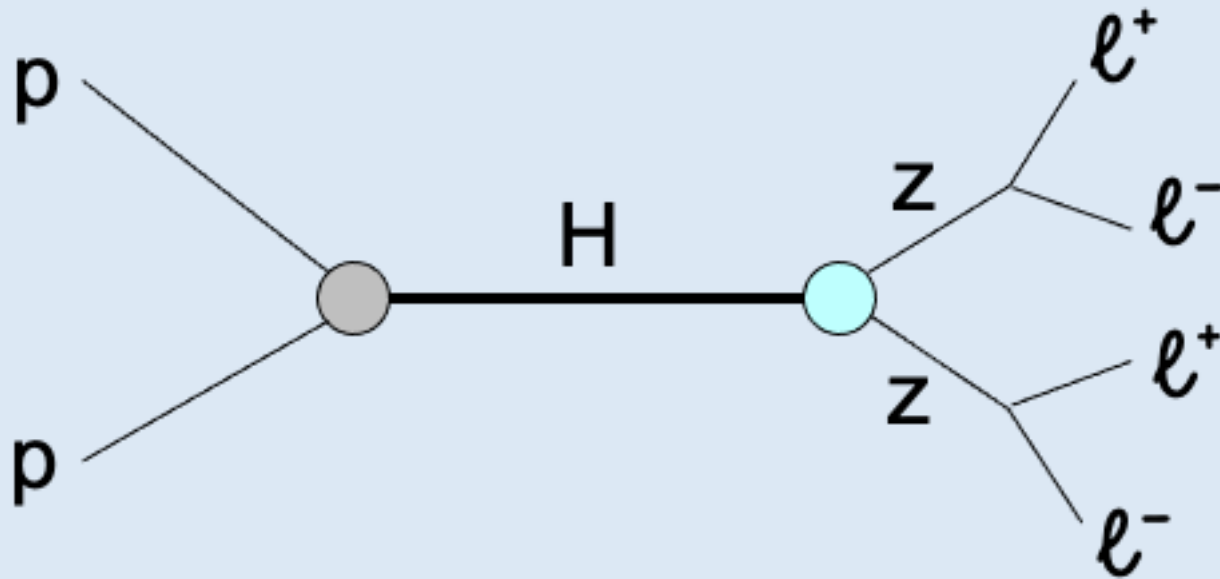
Due to the suppression of the conventional H-width into longitudinal W's and Z's, the relevant production mechanism in our picture is through the Gluon-Gluon Fusion (GGF) process. In fact, the other production through Vector-Boson Fusion (VBF) plays no role. The point is that the $VV \rightarrow H$ process (here $VV = W^+W^-, ZZ$) is the inverse of the $H \rightarrow VV$ decay so that $\sigma^{\text{VBF}}(pp \rightarrow H)$ can be expressed [26] as a convolution with the parton densities of the same Higgs resonance decay width. The importance given traditionally to VBF depends on the conventional large width into longitudinal W's and Z's computed with the $3K^2$ coupling. In our case, where this width is rescaled by the small ratio $(125/700)^2 \sim 0.032$, one finds $\sigma^{\text{VBF}}(pp \rightarrow H) \lesssim 10$ fb which can be safely neglected.

The widths $\Gamma(H \rightarrow WW)$ and $\Gamma(H \rightarrow ZZ)$ are much smaller than conventionally. But new processes...

- $H \rightarrow hh$ $h=h(125)$
- $H \rightarrow hhh, H \rightarrow hWW, H \rightarrow hZZ \dots$
- Due to the H-h overlapping difficult to estimate precisely the total width $\Gamma(H \rightarrow \text{all})$
- Approximately, we expect $\Gamma(H \rightarrow \text{all}) = 30 \div 40 \text{ GeV}$
- Therefore, signatures of the second Higgs resonance:
 - i) mass around 700 GeV
 - ii) produced at LHC mainly through gluon-gluon fusion
 - iii) total width $30 \div 40 \text{ GeV}$

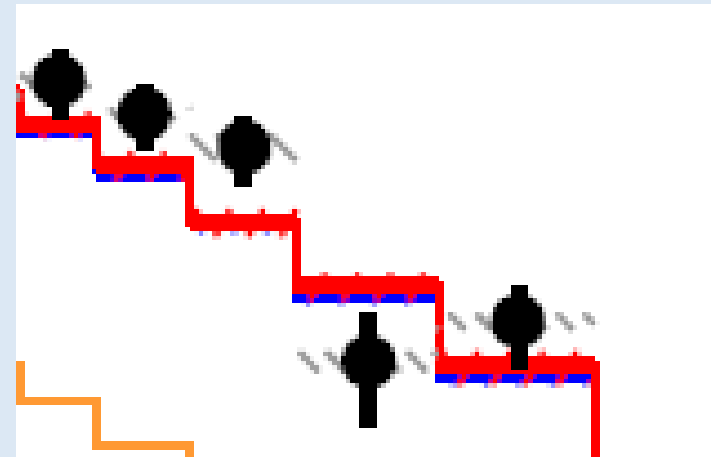
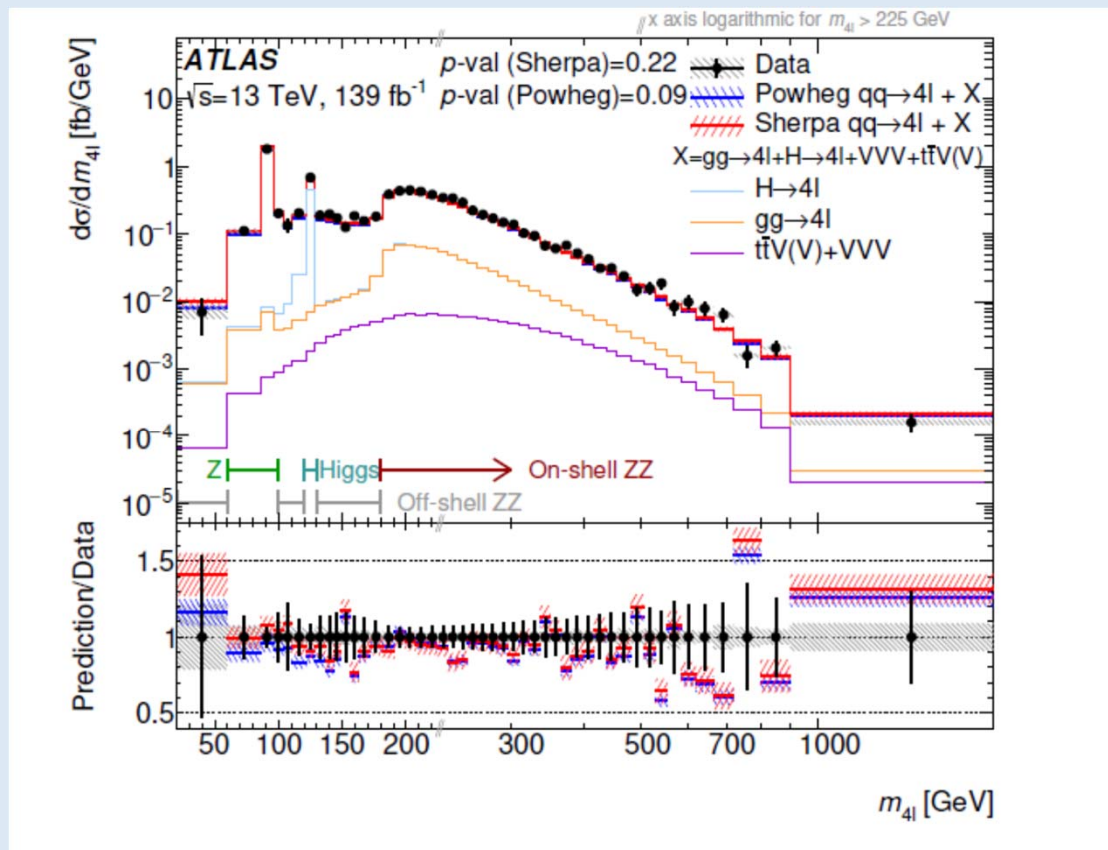
- **Search for experimental signals in the LHC data**
- 1) ATLAS 4-lepton events for invariant mass 560-800 GeV
- 2) ATLAS $\gamma\gamma$ events for invariant mass 600-770 GeV
- 3) CMS (b-b + $\gamma\gamma$) final state
- 4) CMS $\gamma\gamma$ events produced in pp double-diffractive scattering

The process $H \rightarrow 4\text{-leptons}$



ATLAS full 4-lepton cross-section $m_{4l} = 560\div 830$ GeV

see Fig.5 of JHEP 07(2021)005; arXiv:2103.01918v1 [hep-ex]

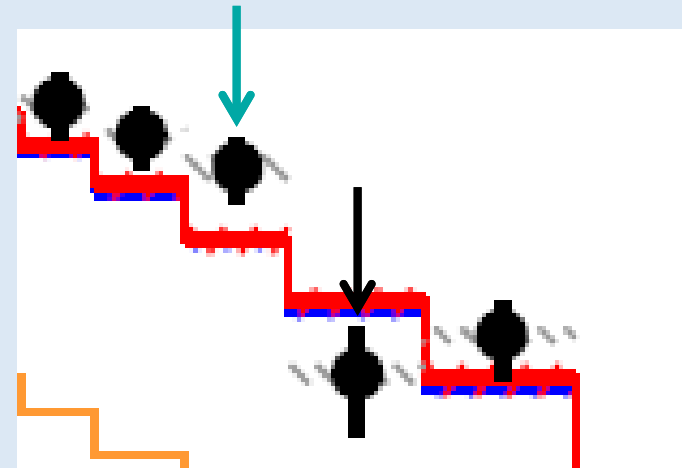
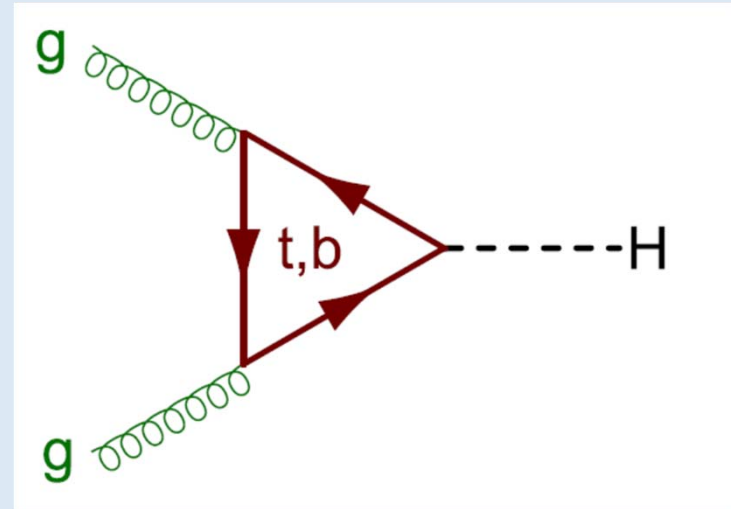


Restricting to gluon-gluon fusion (ggF) events

(Table taken from <https://www.hepdata.net/record/ins1820316>)

Table 1. For luminosity 139 fb^{-1} , we report the observed ATLAS ggF-low events and the corresponding estimated background²⁰ in the range of invariant mass $M_{4l} = E = 530 \div 830 \text{ GeV}$. To avoid spurious fluctuations, due to migration of events between neighbouring bins, we have followed the same criterion as in Fig.5 of ref.²² by grouping the data into larger bins of 60 GeV, centered at 560, 620, 680, 740 and 800 GeV. These were obtained by combining the corresponding 10 bins of 30 GeV, centered respectively at the neighbouring pairs: $545(15) \div 575(15) \text{ GeV}$, $605(15) \div 635(15) \text{ GeV}$, $665(15) \div 695(15)$, $725(15) \div 755(15) \text{ GeV}$ and $785(15) \div 815(15) \text{ GeV}$ as reported in ref.²⁰ In this energy range, the errors in the background are below 5% and will be ignored.

$E[\text{GeV}]$	$N_{\text{EXP}}(E)$	$N_{\text{bkg}}(E)$	$N_{\text{EXP}}(E) - N_{\text{bkg}}(E)$
560(30)	38 ± 6.16	32.0	6.00 ± 6.16
620(30)	25 ± 5.00	20.0	5.00 ± 5.00
680(30)	26 ± 5.10	13.04	12.96 ± 5.10
740(30)	3 ± 1.73	8.71	-5.71 ± 1.73
800(30)	7 ± 2.64	5.97	1.03 ± 2.64



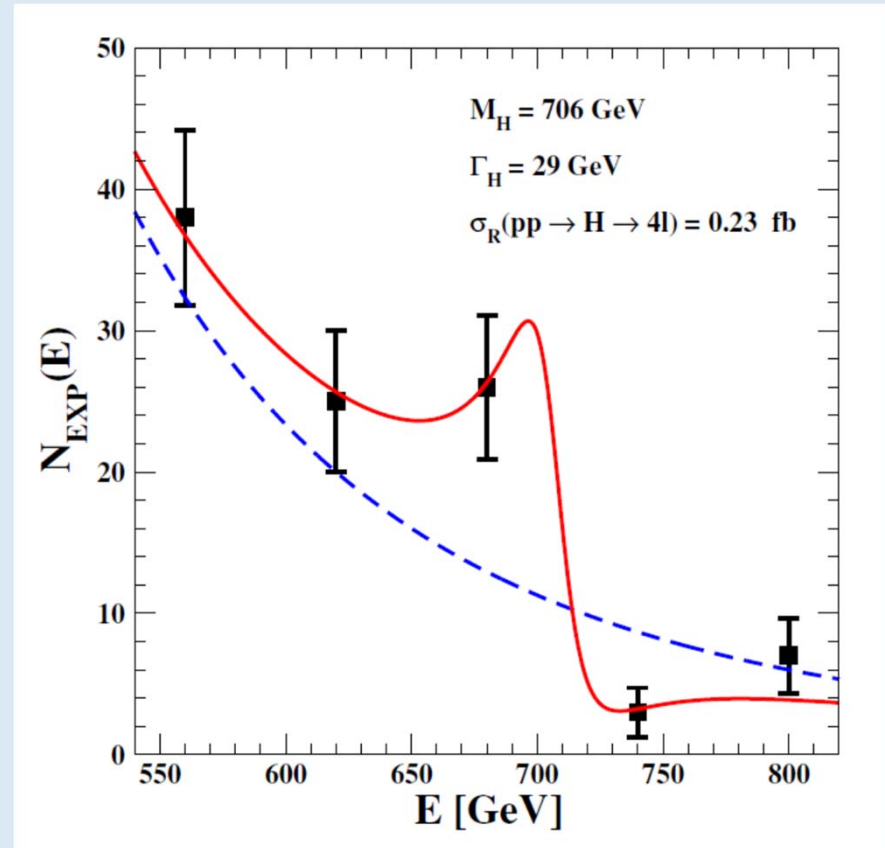
Interpretation

- ATLAS 4-lepton ggF events indicate a $(+2.5\sigma)$ excess in the bin $680(30)$ GeV followed by an opposite (-3.3σ) defect at $740(30)$ GeV
- Simplest interpretation: a resonance with a mass $M_H \approx 700$ GeV which interferes with the background and produces the typical $(M_H^2 - s)$ effect

Background + resonance to describe the ggF-events

Table 2. The experimental ATLAS ggF-low events are compared with our theoretical prediction Eq.(14) for $M_H = 706$ GeV, $\gamma_H = 0.041$, $P = 0.14$.

E[GeV]	$N_{\text{EXP}}(E)$	$N_{\text{TH}}(E)$	χ^2
560(30)	38 ± 6.16	36.72	0.04
620(30)	25 ± 5.00	25.66	0.02
680(30)	26 ± 5.10	26.32	0.00
740(30)	3 ± 1.73	3.23	0.02
800(30)	7 ± 2.64	3.87	1.40



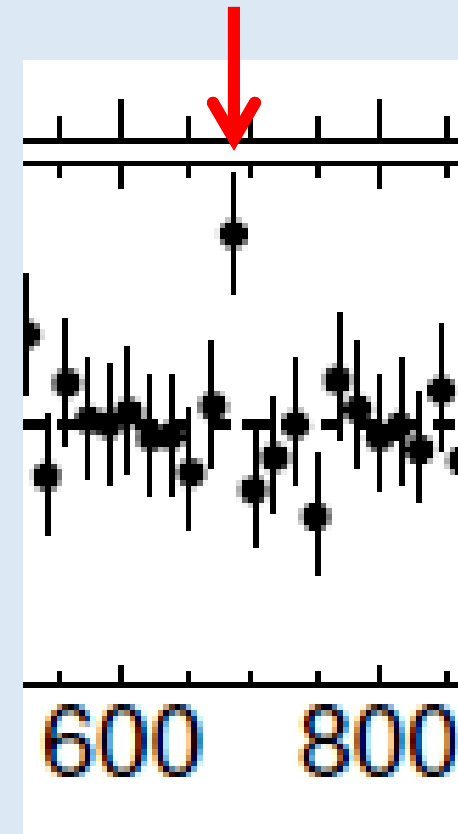
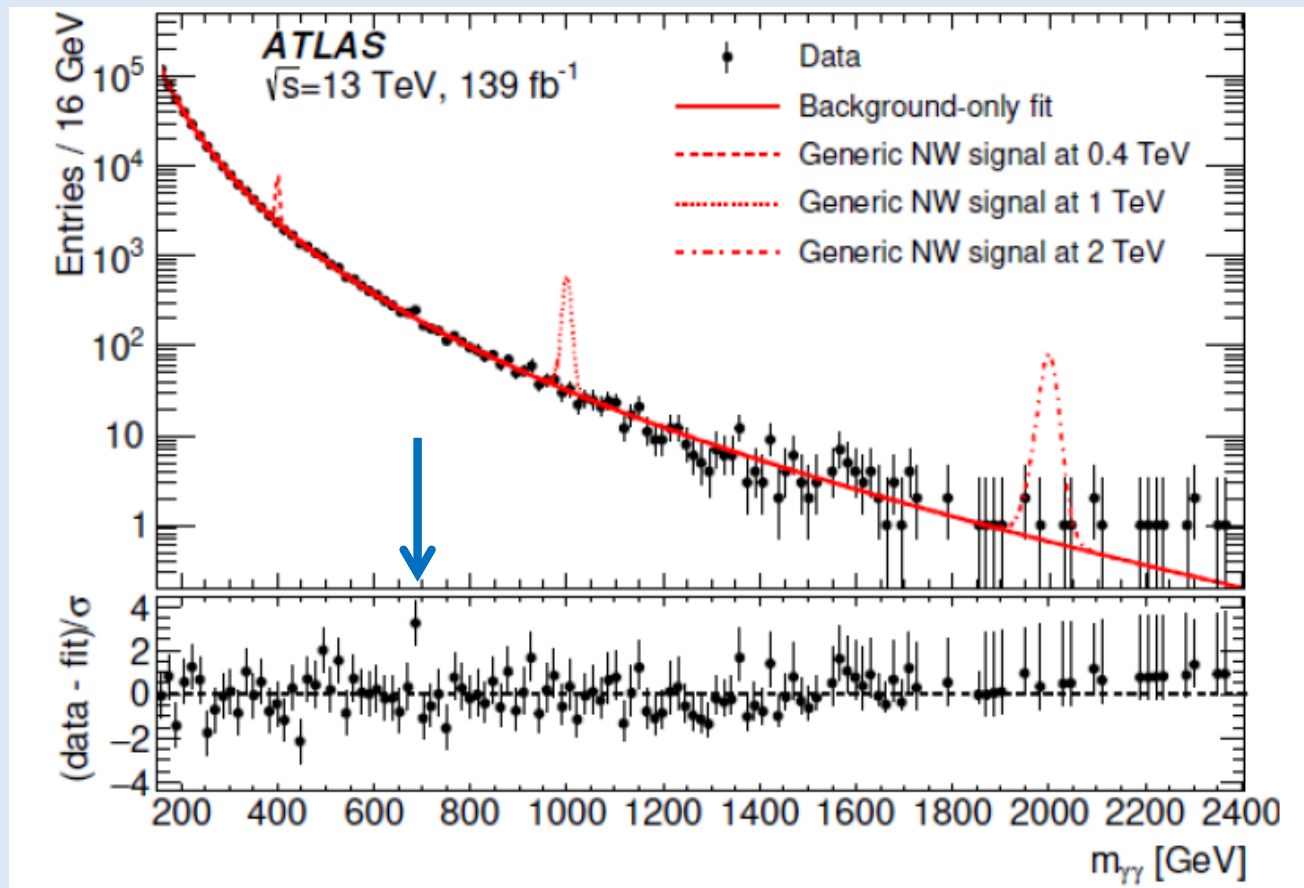
- **Red continuous line = background + resonance**
- **Blue dashed line = ATLAS background only**

More signals in the same mass region

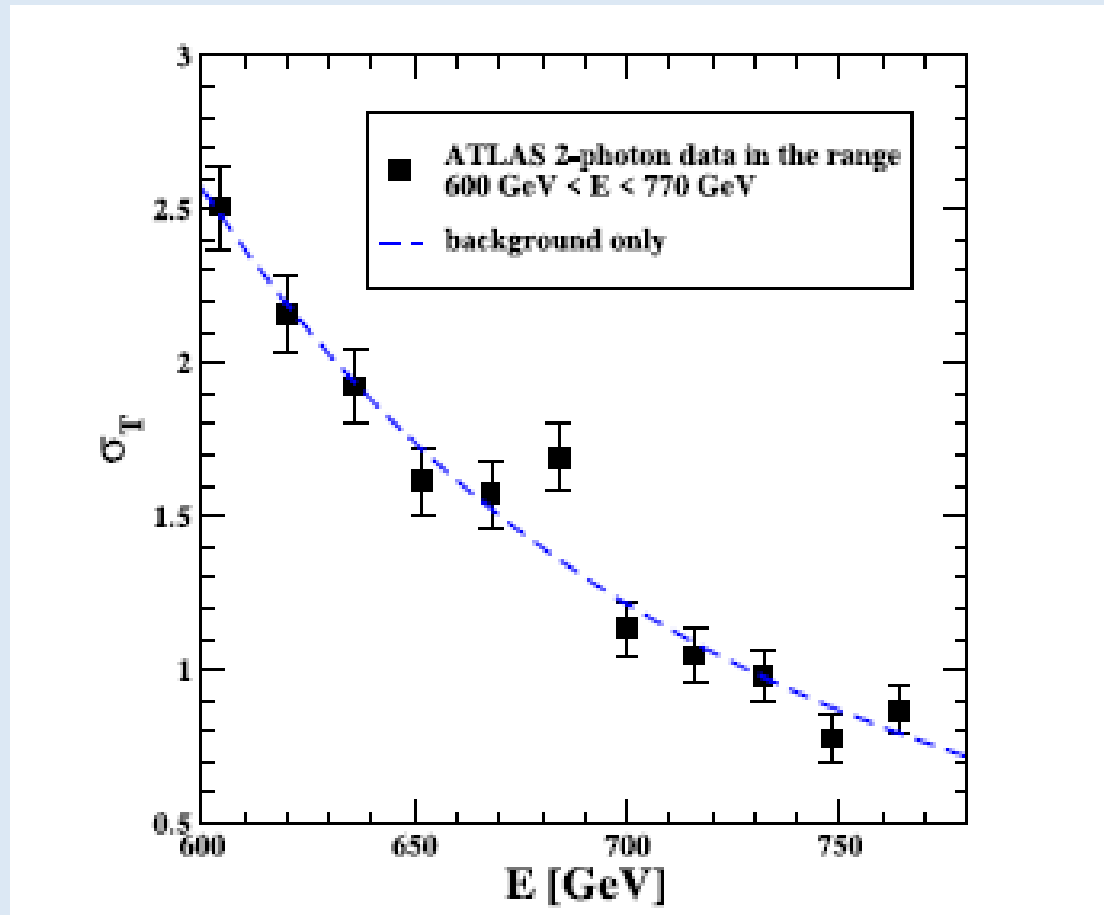
- i) ATLAS high-mass $\gamma\gamma$ events
- ii) CMS search for a new state X through the chain
$$pp \rightarrow X \rightarrow h(125) + h(125) \rightarrow (b\text{-}b + \gamma\gamma)$$
- iii) CMS search for high mass $\gamma\gamma$ pairs produced in pp double-diffractive scattering
$$pp \rightarrow p + X + p$$
and then $X \rightarrow \gamma\gamma$

ATLAS $\gamma\gamma$ spectrum: a (local) 3.3σ excess at $E=684$ GeV

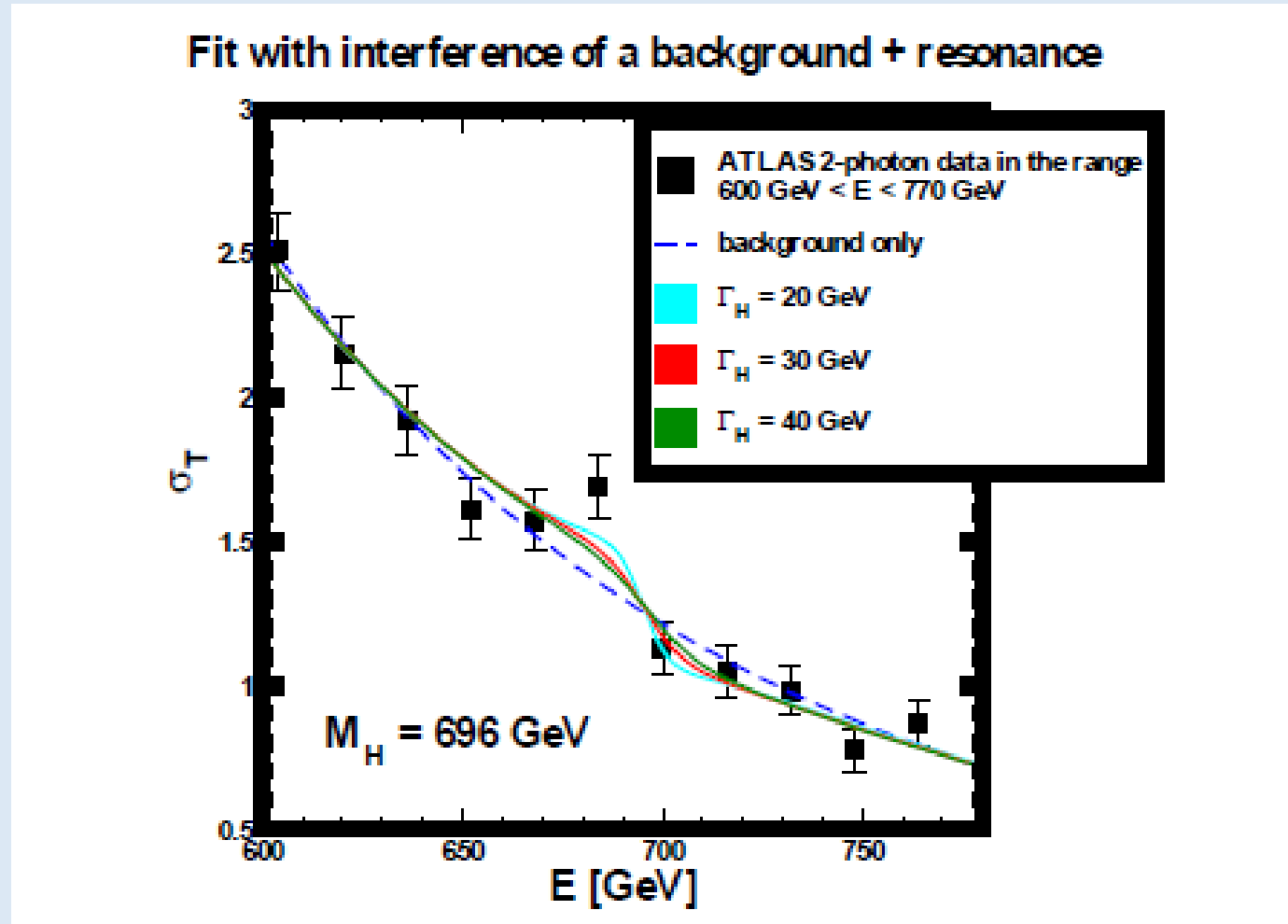
see ATLAS Coll. PLB 822 (2021) 136651



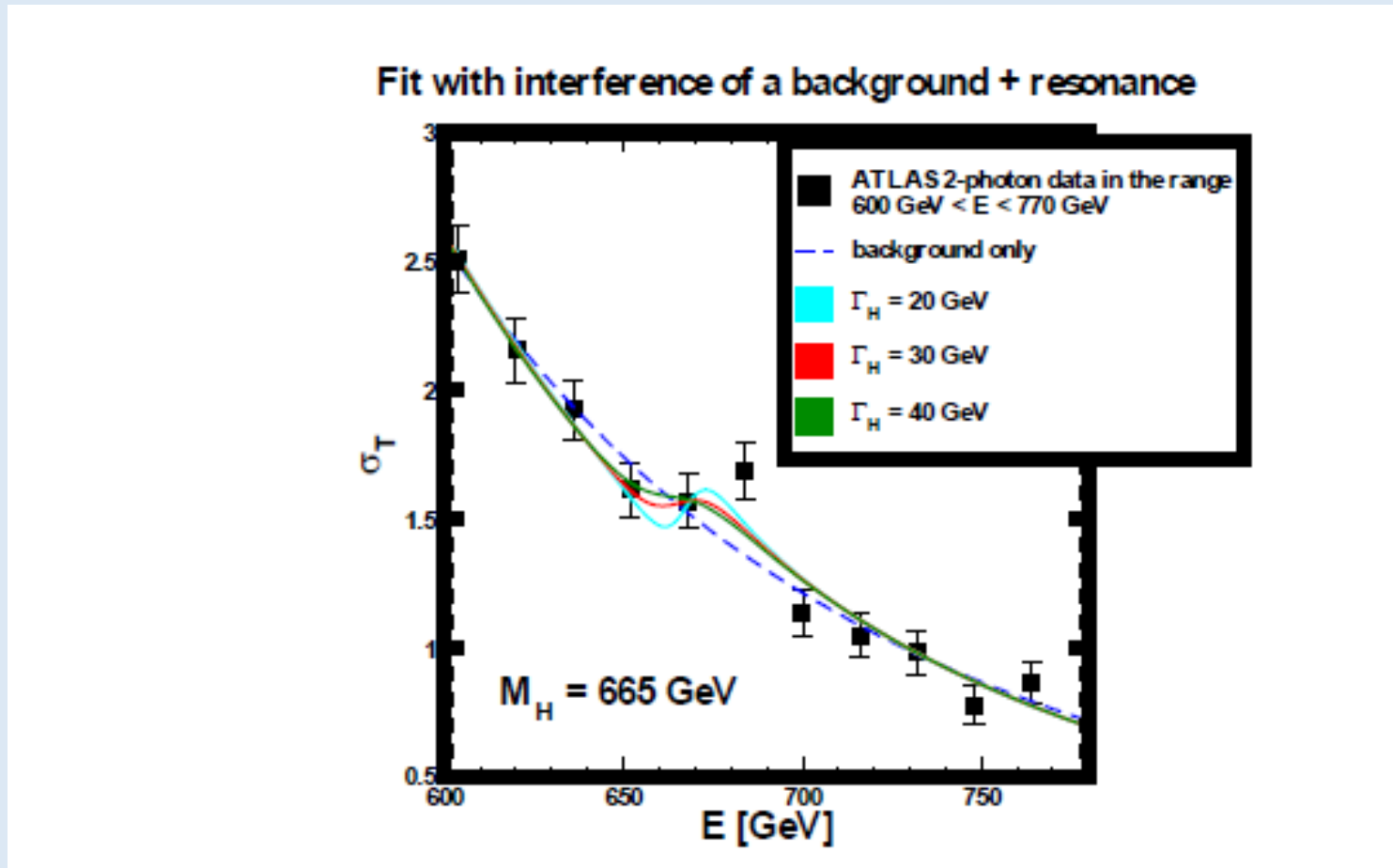
Fit to ATLAS $\gamma\gamma$ with background only ($\chi^2=14$)



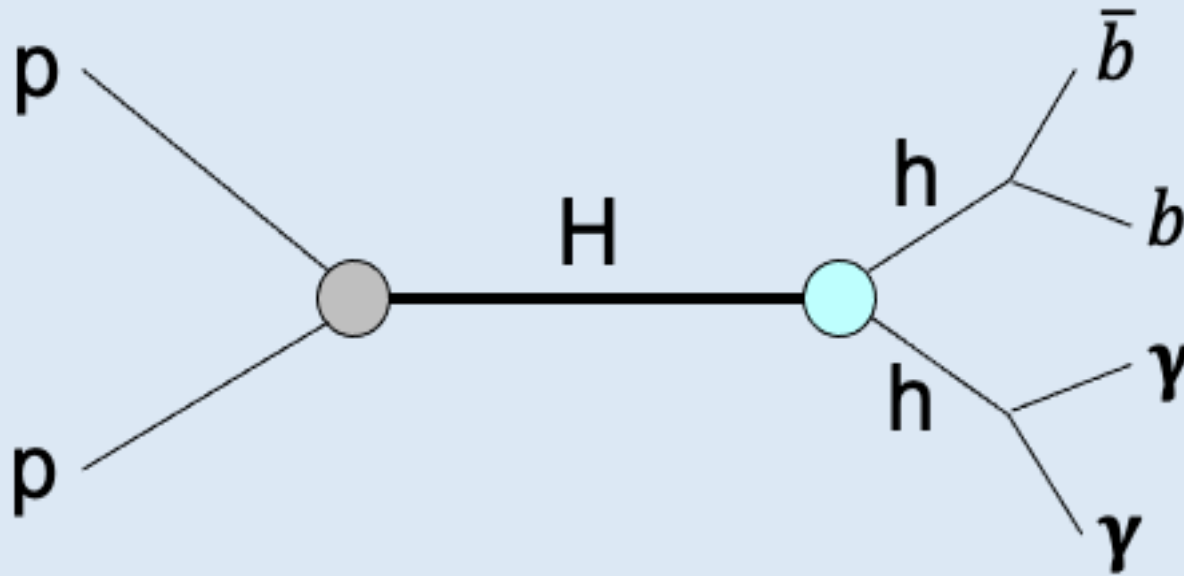
Fit to ATLAS $\gamma\gamma$ with positive interference ($\chi^2 = 8 \div 11$)



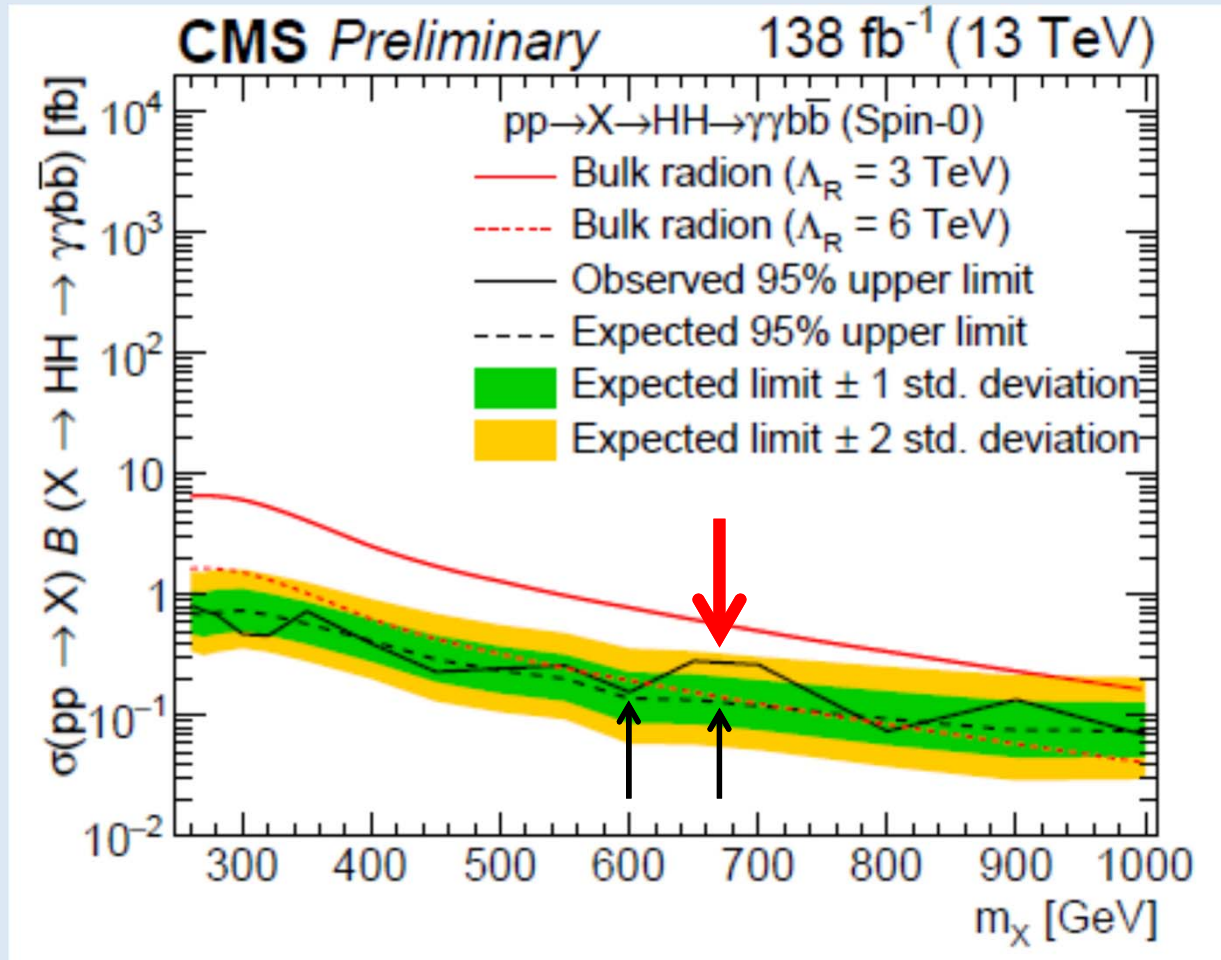
Fit to ATLAS $\gamma\gamma$ with negative interference ($\chi^2 = 9 \div 12$)



The process $X=H \rightarrow h(125)+h(125) \rightarrow 2b\text{-quark jets} + \gamma\gamma$

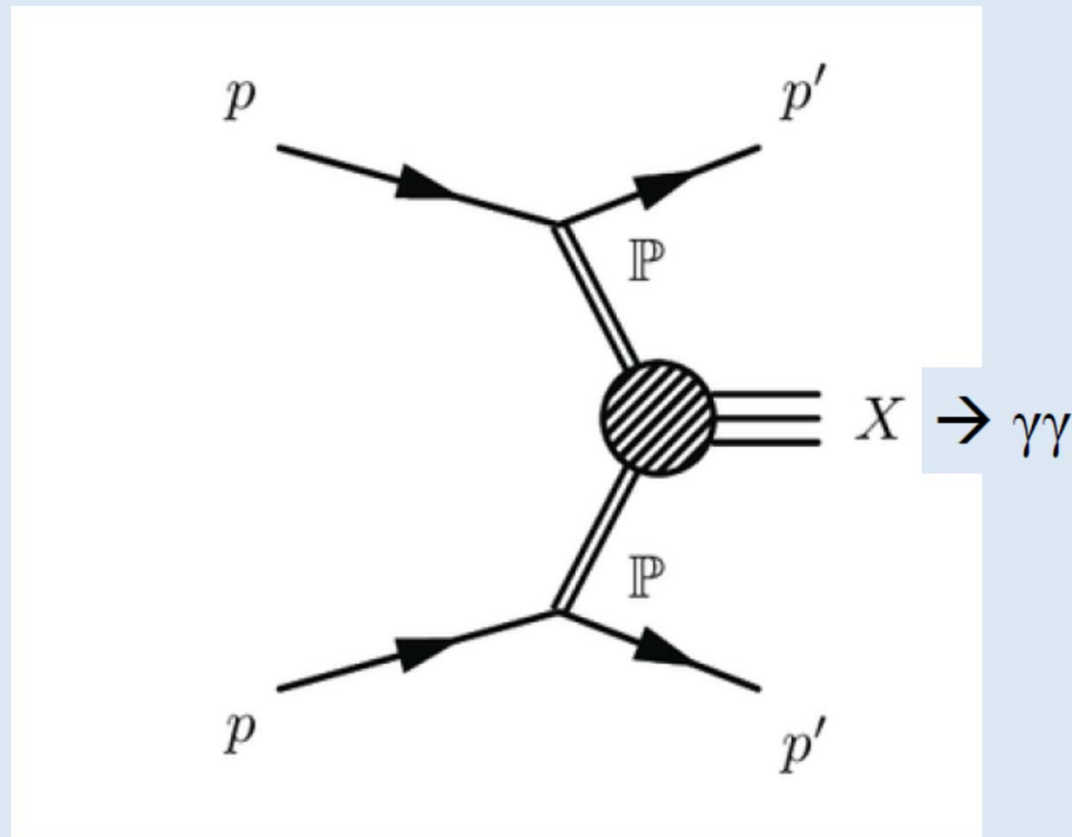


CMS analysis of the cross section for the process $pp \rightarrow X \rightarrow h(125)+h(125) \rightarrow (b\text{-}b + \gamma\gamma)$ (Report CMS-PAS-HIG-21-011)

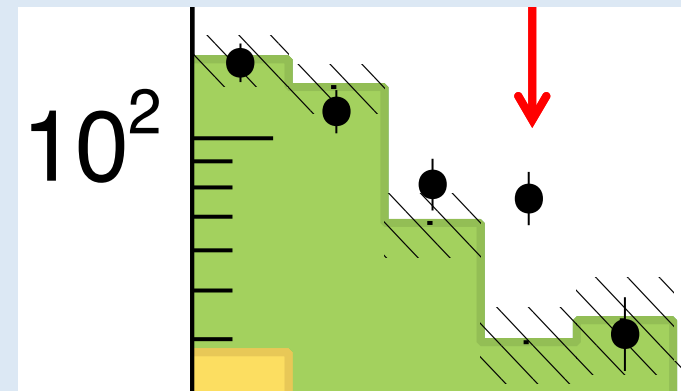
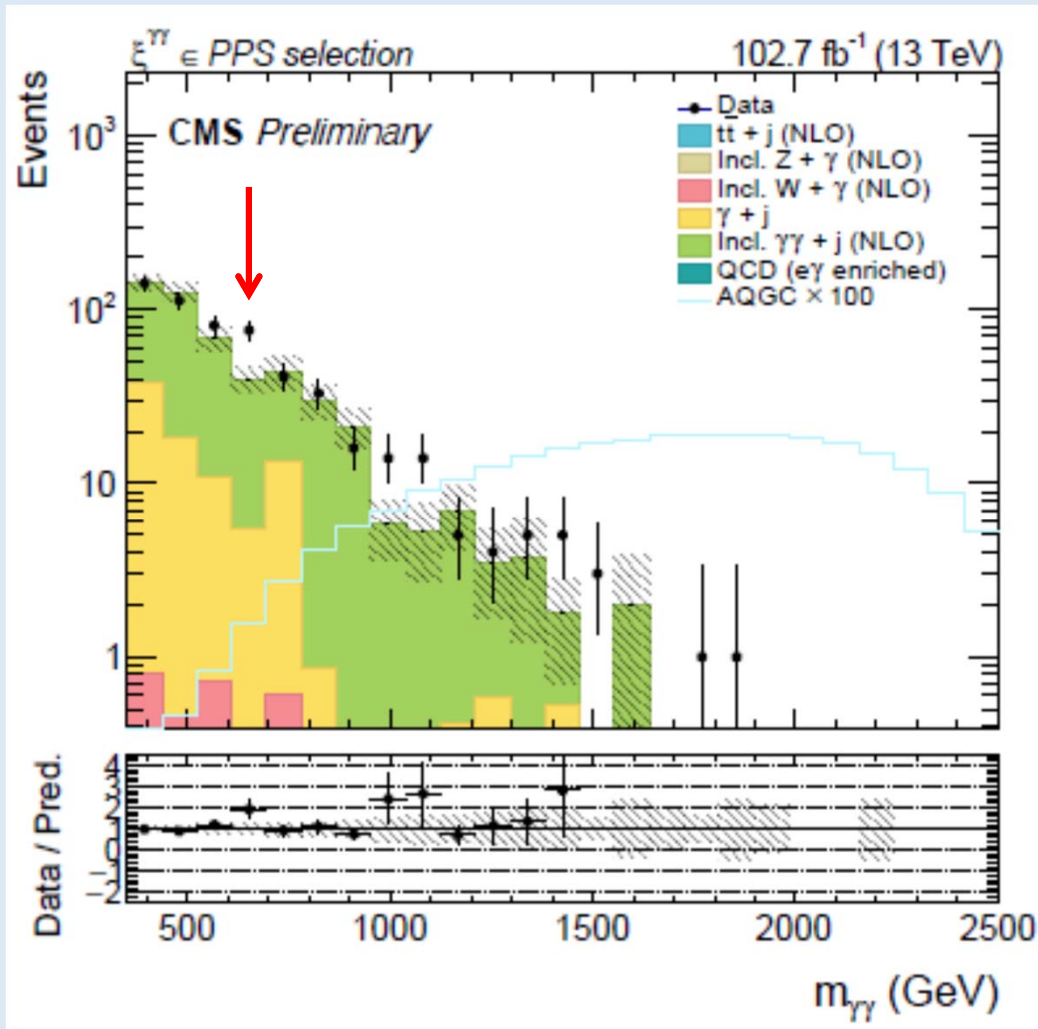


- At 600 GeV, observed and estimated 95% CL coincide for a value 0.16 fb
- In the **plateau 675(25) GeV**, the limit placed by the observed number of events is 0.30 fb, about twice the expected background with a 1.6 σ excess

**Double-diffractive pp scattering producing a state $X \rightarrow \gamma\gamma$
with the same quantum numbers of the vacuum**
(«Diffractive excitation of the vacuum» M.Albrow, arXiv:1010.0625 [hep-ex])



CMS analysis of $\gamma\gamma$ produced in pp double-diffractive scattering (Report CMS-TOTEM Coll. CMS-PAS-EXO-21-007)



- For a $m(\gamma\gamma) = 650(40)$ GeV \rightarrow 76(9) events OBSERVED vs. 40(6) EXPECTED
- In the most conservative case this is a 3.3 σ effect (the only significant excess)

- **Conclusions:** having a prediction $(M_H)^{\text{THEOR}} = 690 \pm 10 \text{ (stat)} \pm 20 \text{ (sys) GeV}$, local excesses (or local defects) should maintain intact their statistical significance and not be downgraded by the “look elsewhere” effect
- Therefore, the correct perspective is that we are faced with :
 - i) a **2.5- σ** excess AND a **3.3- σ** defect around **700 GeV** in the ATLAS 4-leptons
 - ii) a **3.3 σ** excess at **684(8) GeV** in the ATLAS $\gamma\gamma$ channel
 - iii) a **1.6 σ** excess at **675(25) GeV** in the CMS (b-b+ $\gamma\gamma$) channel
 - iv) a **3.3 σ** excess at **650(40) GeV** in the CMS exclusive $\gamma\gamma$ produced in pp double-diffractive scattering
- The correlation of these measurements is very small. One could argue that the cumulated statistical evidence for a new (relatively narrow) resonance

$$(M_H)^{\text{EXP}} \sim 700 \text{ GeV}$$

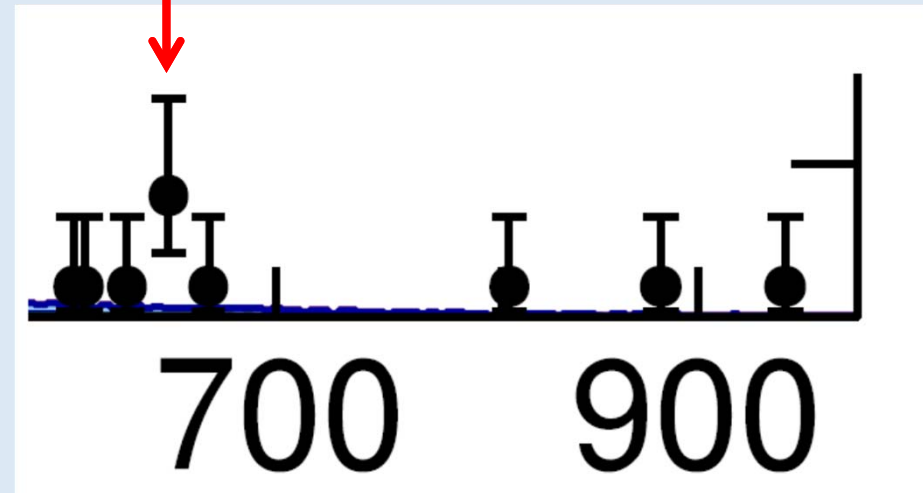
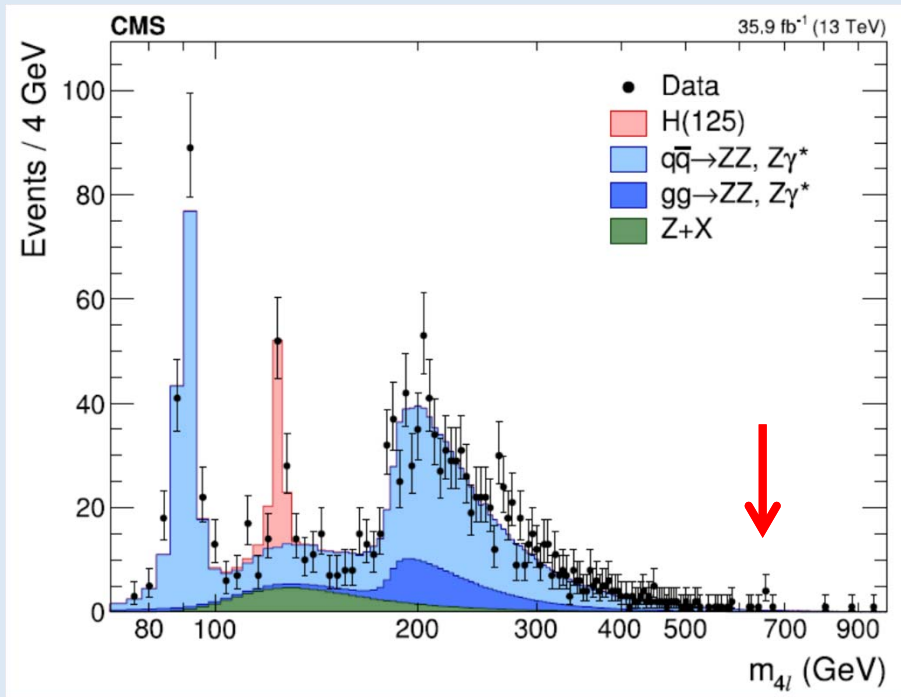
has reached the traditional **5 σ** discovery level

Of course, also systematic uncertainties, but \rightarrow **present situation is unstable**

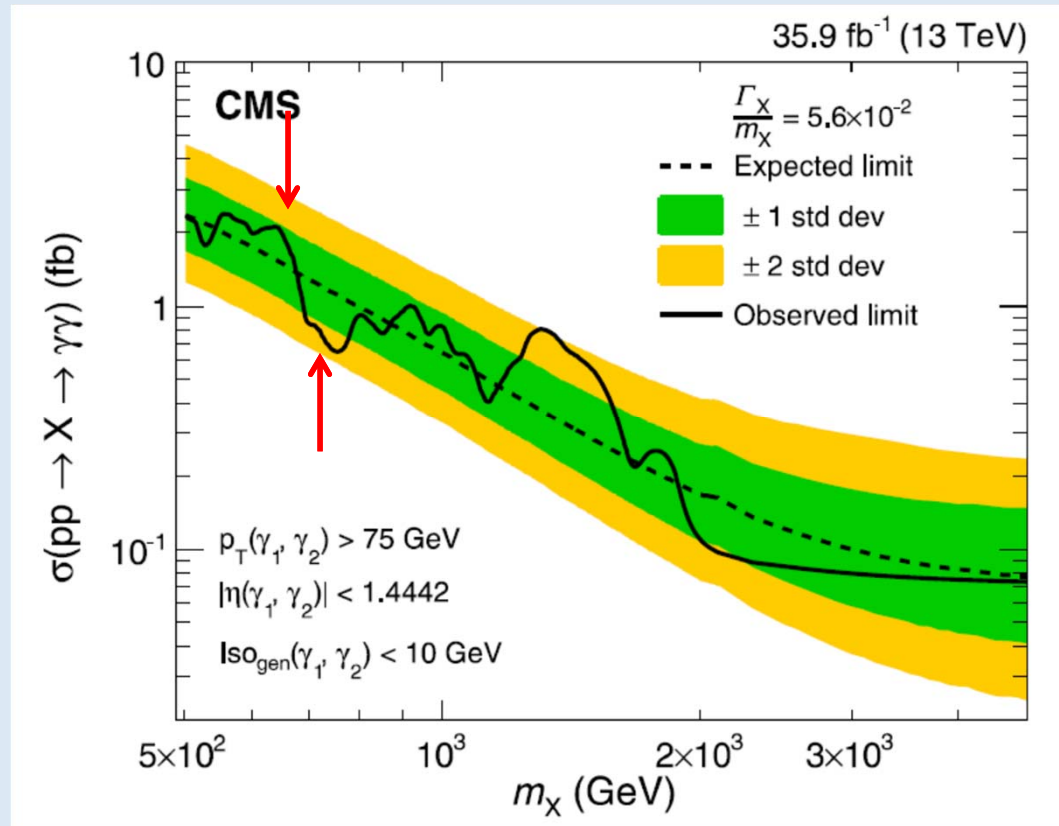
It could soon be resolved with two crucial missing samples from RUN2:

- a) full **CMS** invariant-mass data for the **charged 4-lepton channel**
- b) full **CMS** invariant-mass data for the **inclusive $\gamma\gamma$ channel**

Low-statistics partial CMS results: 4-leptons



Low-statistics partial CMS results: inclusive $\gamma\gamma$



- A 1- σ excess at 640(30) GeV followed by a 1.5-sigma defect at 750(40) GeV. (same qualitative pattern as present ATLAS 4-leptons, with much less statistics)

A remark on radiative corrections

- With two resonances of the Higgs field, what about radiative corrections?
- Our lattice simulations indicate a propagator structure

$$G(p) \sim \frac{1 - I(p)}{2} \frac{1}{p^2 + m_h^2} + \frac{1 + I(p)}{2} \frac{1}{p^2 + M_h^2} \quad (4)$$

with an interpolating function $I(p)$ which depends on an intermediate momentum scale p_0 and tends to $+1$ for large $p^2 \gg p_0^2$ and to -1 when $p^2 \rightarrow 0$.

- This is very close to van der Bij propagator [Acta Phys. Polon. B11 \(2018\) 397.](#)

$$(-1 \leq \eta \leq 1)$$

$$G(p) \sim \frac{1 - \eta}{2} \frac{1}{p^2 + m_h^2} + \frac{1 + \eta}{2} \frac{1}{p^2 + M_H^2} \quad (49)$$

- In the ρ -parameter at one loop, this is similar to have an effective Higgs mass

$$m_{\text{eff}} \sim \sqrt{m_h M_H} (M_H / m_h)^{\eta/2} \quad (47)$$

In our case, this would be between $m_h = 125$ GeV and $M_H \sim 700$ GeV.

- How well, the mass from radiative corrections agree with the direct LHC result 125 GeV?

From the PDG review: positive M_H - $\alpha_s(M_Z)$ correlation (Important: NuTeV is not considered \rightarrow larger M_H)

32 10. Electroweak model and constraints on new physics

Table 10.7: Values of \hat{s}_Z^2 , s_W^2 , α_s , m_t and M_H [both in GeV] for various data sets. In the fit to the LHC (Tevatron) data the α_s constraint is from the $t\bar{t}$ production [204] (inclusive jet [205]) cross-section.

Data	\hat{s}_Z^2	s_W^2	$\alpha_s(M_Z)$	m_t	M_H
All data	0.23122(3)	0.22332(7)	0.1187(16)	173.0 ± 0.4	125
All data except M_H	0.23107(9)	0.22310(19)	0.1190(16)	172.8 ± 0.5	90_{-16}^{+17}
All data except M_Z	0.23113(6)	0.22336(8)	0.1187(16)	172.8 ± 0.5	125
All data except M_W	0.23124(3)	0.22347(7)	0.1191(16)	172.9 ± 0.5	125
All data except m_t	0.23112(6)	0.22304(21)	0.1191(16)	176.4 ± 1.8	125
M_H, M_Z, Γ_Z, m_t	0.23125(7)	0.22351(13)	0.1209(45)	172.7 ± 0.5	125
LHC	0.23110(11)	0.22332(12)	0.1143(24)	172.4 ± 0.5	125
Tevatron + M_Z	0.23102(13)	0.22295(30)	0.1160(45)	174.3 ± 0.7	100_{-26}^{+31}
LEP	0.23138(17)	0.22343(47)	<u>0.1221(31)</u>	182 ± 11	274_{-152}^{+376} 
SLD + M_Z, Γ_Z, m_t	0.23064(28)	0.22228(54)	<u>0.1182(47)</u>	172.7 ± 0.5	38_{-21}^{+30} 
$A_{FB}^{(b,c)}, M_Z, \Gamma_Z, m_t$	0.23190(29)	0.22503(69)	<u>0.1278(50)</u>	172.7 ± 0.5	348_{-124}^{+187} 
$M_{W,Z}, \Gamma_{W,Z}, m_t$	0.23103(12)	0.22302(25)	<u>0.1192(42)</u>	172.7 ± 0.5	84_{-19}^{+22} 
low energy + $M_{H,Z}$	0.23176(94)	0.2254(35)	0.1185(19)	156 ± 29	125

First remark: NuTeV not included by PDG

The NuTeV collaboration found $s_W^2 = 0.2277 \pm 0.0016$ (for the same reference values), which was 3.0σ higher than the SM prediction [89]. However, since then several groups have raised concerns about interpretation of the NuTeV result, which could affect the extracted $g_{L,R}^2$ (and thus s_W^2) including their uncertainties and correlation. These include the assumption of symmetric strange and antistrange sea quark distributions, the electron neutrino contamination from K_{e3} decays, isospin symmetry violation in the parton distribution functions and from QED splitting effects, nuclear shadowing effects, and a more complete treatment of EW and QCD radiative corrections. A more detailed discussion and a list of references can be found in the 2016 edition of this *Review*. The precise impact of these effects would need to be evaluated carefully by the collaboration, but in the absence of a such an effort we do not include the ν DIS constraints in our default set of fits. 

Second remark: the importance of $\alpha_s(M_Z)$

Schmitt → present most complete analysis

hep-ex/0401034
nuhep-exp/04-01

Apparent Excess in $e^+e^- \rightarrow$ hadrons

Michael Schmitt

Northwestern University

January 22, 2004

Abstract

We have studied measurements of the cross section for $e^+e^- \rightarrow$ hadrons for center-of-mass energies in the range 20–209 GeV. We find an apparent excess over the predictions of the Standard Model across the whole range amounting to more than 4σ .

Higgs mass from LEP1

TOKUSHIMA 95-02
(hep-ph/9503288)
March 1995

Remarks on the Value of the Higgs Mass
from the Present LEP Data

M. CONSOLI^{a)} AND Z. HIOKI^{b)}

ABSTRACT

We perform a detailed comparison of the present LEP data with the one-loop standard-model predictions. It is pointed out that for $m_t = 174$ GeV the “bulk” of the data prefers a rather large value of the Higgs mass in the range 500-1000

ALEPH+DELPHI+L3+OPAL

α_s	0.113	0.125	0.127	0.130
$m_h(\text{GeV})$	100	100	500	1000
TOTAL χ^2	43.6	37.8	36.4	38.2

Table VII. Total χ^2 for the four Collaborations.

α_s	0.113	0.125	0.127	0.130
$m_h(\text{GeV})$	100	100	500	1000
ALEPH	6.7	8.6	7.6	8.2
DELPHI	7.6	8.8	7.3	7.3
L3	10.3	4.7	5.4	5.9
OPAL	11.4	7.9	5.1	4.1
TOTAL χ^2	36.0	30.0	25.4	25.5

Table VIII. Total χ^2 for the four Collaborations by excluding the data for $A_{FB}^0(\tau)$.